Neuroprotection of Extracellular Vesicles From Human Adipose Stem Cells Intranasally Administered 24 Hours After Stroke In Rats

Francieli Rohden (franrohden@gmail.com)
UFRGS: Universidade Federal do Rio Grande do Sul https://orcid.org/0000-0002-9232-7371
Luciele Varaschini Teixeira
Universidade Federal do Rio Grande do Sul
Luis Pedro Bernardi
Universidade Federal do Rio Grande do Sul
Pâmela Cristina Lukasewicz Ferreira
Universidade Federal do Rio Grande do Sul
Mariana Colombo
Universidade Federal do Rio Grande do Sul
Geciele Rodrigues Teixeira
HCPA: Hospital de Clinicas de Porto Alegre
Fernanda dos Santos de Oliveira
HCPA: Hospital de Clinicas de Porto Alegre
Elizabeth Obino Cirne Lima
HCPA: Hospital de Clinicas de Porto Alegre
Fátima Rodrigues Guma
Universidade Federal do Rio Grande do Sul
Diogo Onofre Souza
Universidade Federal do Rio Grande do Sul https://orcid.org/0000-0002-4322-0404

Research Article

Keywords: human adipose tissue mesenchymal stem cells, extracellular vesicles, experimental ischemic stroke, intranasal treatment, neuroprotection

Posted Date: March 1st, 2021

DOI: https://doi.org/10.21203/rs.3.rs-249331/v1

Abstract

Ischemic stroke is a prominent cause of death and disability, demanding for innovative and reachable therapeutic strategies. Thus, approaches presenting optimal period for therapeutic intervention and new routes of treatments administration as promising tools for stroke treatment. In this study, we evaluated the potential neuroprotective properties of nasally administration of human adipose tissue stem cells (hAT-MSC)-derived extracellular vesicles (EVs), obtained from healthy individuals submitted to liposuction. A single intranasal EVs (200 µg/Kg) administration performed 24 h after a focal permanent ischemic stroke in rats. Was observed a higher tropism of EVs by peri-infarct zone, surrounding the infarct core. Interestingly, in the same brain region, was observed a significant decrease in the volume of the infarct, improvement the blood-brain barrier and re-stabilization of vascularization. In addition, EVs recover the impairment on long-term motor and behavioral performance induced by ischemic stroke. Surprisingly, one single intranasal EVs administration reestablished: i) front paws symmetry; ii), short- and long-term memory; iii) anxiety-like behavior. In keeping with this, our work highlights hAT-MSC-derived EVs as a promising therapeutic strategy in stroke.

Introduction

Stroke is a prominent cause of death and permanent disability worldwide, impacting health and financial burden [1, 2]. Ischemic stroke represents ~ 85% of stroke cases [3–6], in which approximately 80% cause contralateral upper limb paresis [7] and sensory function impairment [8]. In addition, clinical observations show that 20–50% of patients experience memory disorders [9, 10].

The ischemic stroke pathophysiology is characterized by blood flow obstruction of a restricted brain region, forming an infarct nucleus, surrounded by an area known as penumbra region. Of note, this region has the potential to be reperfused [11] and in animals models refers as the peri-infarct region [12]. Reperfusion of the penumbra/peri-infarct zone contributes to a reduction in the final infarct size and attenuation/reversal of neurological and behavioral deficits [13, 14]. Therefore, therapeutic strategies with focus on penumbra region salvage are intensively searched [15]. Currently, the gold standard treatment for ischemic stroke is the use of thrombolytic agents, which focuses on optimizing the reperfusion time in the penumbra region [16]. However, this strategy has to be strictly applied within 4.5 h after the first symptoms [17]. In addition, reperfusion injury, such as hemorrhage, is the most dangerous collateral effect after thrombolysis [18, 19]. Thus, the thrombolytic treatment is contraindicated for a certain class of patients at risk for bleeding or for the formation of large blood clots [20]. Additionally, some patients would be considered for endovascular therapy (Mechanical Thrombectomy), which could increase the maximum time to receive treatment up to 24h after first symptoms; however, this procedure requires qualified professionals and infrastructure to conduct imaging exams (computed tomography scan and angiogram computed tomography)[18, 21].

Therefore, it is essential to find new and accessible therapeutic strategies for ischemic stroke. In vivo studies using rat models of brain ischemia demonstrated that treatment with mesenchymal stem cells

(MSCs) increased the therapeutic window up to 24 h after insult [22–24]. Though MSCs therapy seems very promising, it may cause some impacting damage such as immune system rejection and increased risk of developing tumor tissue [25]. In this way, improvements in MSC therapy have been made to optimize its efficacy. It is currently thought that MSCs protective effects are due to the release of extracellular vesicles (EVs). The EVs are small double membrane vesicles (30-200nm), released by many cell types, which in physiological conditions mediate cell-to-cell communication [26]. Compared to MSCs, EVs have lower immunogenicity, decreasing the risk of obstructive vascular effect and of secondary microvascular thrombosis and presenting higher ability to cross the blood-brain barrier (BBB) [27, 28].

Previous experimental studies systemically administrating EVs 24h after ischemic stroke demonstrate increased angiogenesis, neurogenesis, neurite remodeling, with a long-term recovery in rats [29–32]. However, EVs systemically administered may undergo metabolization before reaching the brain tissue [33], being detected in other organs (such as lungs, liver and spleen)[34]. Thus, some studies are focusing on a straightforward and noninvasive strategy to administer EVs targeting the brain, as a potential strategy to treat brain disorders [35–37].

In this study, we investigated the neuroprotective effects of EVs released from human adipose tissue mesenchymal stem cell (hAT-MSCs), through a single intranasal administration 24 h after ischemic injury in rats. In specific, we evaluated short- and long-term effects of a permanent focal stroke model and the EVs effects on forepaws symmetry, behavioral performance, anxiety-like behavior, brain infarct volume, BBB permeability and brain formation of new blood vessels.

Materials And Methods

1. **hAT-MSCs: sources, culture and characterization.**

The cells were obtained from commercial and human sources

1a. Commercial hAT-MSCs.

Cells were obtained from the POIETICS bank - Adipose-Derived Stem Cells (cat. #PT-5006, donor 34464. The cell type was confirmed by the presence of clusters of differentiation (CDs) such as CD13, CD29, CD44, CD73, CD90, CD105 and CD166, and by the absence of CDs such as CD14, CD31 and CD45. They were tested negatively for mycoplasma, bacteria, yeast and fungi by the supplier company. A frozen vial containing ~ $1x10^6$ cells was thawed at 37ºC and plated in 25 cm^2 flask (TPP). Cells were cultured with DMEM medium (Sigma) containing 10% FBS (Cripion), 100 units/mL penicillin (Gibco), 100 µg/mL streptomycin (Gibco), 50 mg/L gentamicin (Sigma) and 2.5 mg/L fungizone (Sigma). After 24 hours, debris and non-adherent cells were gently removed [36]. When adherent cells reached 80% confluence (passage1: P1), hADSCs were detached with 0.25% trypsin/1 mM ethylenediamine tetra acetic acid (EDTA) (Sigma) and plated in flasks at a density of $1,5×10^4$ cells/75 cm^2 (passage 2: P2). The cellular density was determined by manually counting the number of cells at each passage[38]. The cells are

named as cell 0 (C0). C0 were expanded under the above-described conditions and used only from 4th to 8th passage [29, 38, 39].

1b. Patient-derived hAT-MSCs

Cells were obtained from the subcutaneous adipose tissue of two 30-year-old females submitted to abdominal liposuction at the Hospital de Clínicas in Porto Alegre (University Hospital), RS, Brazil. The patients agreed to participate in the research and signed a consent form (GPPG 2018 – 0374). The fresh adipose tissue was washed with PBS buffer, minced and digested for 1 h in 0.1% collagenase at 37°C. The digestion process was stopped by the addition of Dulbecco's Modified Eagle's Medium (DMEM) containing 20% fetal bovine serum (FBS) and 100 units/mL penicillin (Gibco), 100 µg/mL streptomycin (Gibco). The digested suspension was filtered through a 70 µm nylon mesh cell filter to retain the tissue debris. The filtered suspension was centrifuged at 400×g for 5 min. The stromal vascular fraction (pellet) was resuspended in DMEM + 20% FBS (Cripion) medium and cultured in flasks cell culture of 25 mc^2 (TPP) at 37°C in a humidified atmosphere of 5% CO_2. After 24 hours, the non-adherent cells were gently removed[38]. When adherent cells reached 80% confluence (passage 0: P0), confluent cells (hAT-MSCs) were detached with 0.25% trypsin/1 mM ethylenediamine tetra acetic acid (EDTA) (Sigma) and plated in flasks at a density of $1{,}5\times10^4$ cells/75 cm^2 (TPP) (passage1: P1). Cells were cultured with DMEM medium (Sigma) containing 10% FBS (Cripion) and 100 units/mL penicillin (Gibco), 100 µg/mL streptomycin (Gibco), gentamicin 50mg/L (Sigma) and fungizone 2.5mg/L (Sigma). These cells are named as cell 1 – patient 1 (C1) and cell 2 – patient 2 (C2). C1 and C2 were expanded under the same above-described conditions and used only from 4th to 8th passage[35, 39].

C1 and C2 hAT-MSCs were characterized by immune fluorescence through flow cytometry and confocal microscopy.

Flow cytometry: hAT-MSCs were centrifuged (400×g for 5 min at room temperature), the cell pellet was resuspended in DMEM + 10% FBS and the cells were counted in a Neubauer chamber. Shortly after, cells were incubated with antibodies at concentration of 1:50 for 4 h at 37°C. Then, cell suspensions were centrifuged at 400×g for 5 min at room temperature, and cell pellets resuspended in 200 µl of PBS. Ten thousand events were analyzed using flow cytometry (BD FACSCalibur™)[40]. Cells, only in passage 4 (P4), were characterized as hAT-MSCs by CDs presence: CD34 (FITC Mouse Anti-human CD34 BD Pharmingen), CD45 (Human CD45 FITC Conjugate, Invitrogen), CD90 (PE Mouse Anti-Human CD90 BD Pharmingen) and CD105 (Huan CD105 R-PE conjugate, Invitrogen).

Confocal microscopy: an aliquot of $1x10^4$ hAT-MSCs was placed on a slide and analyzed by immunofluorescence. Cells were maintained in culture conditions for 72 h to adhere to the coverslip. Then, cells were incubated for 4 h at 37°C with the same antibodies used for cytometry: CD34, CD45, CD90 and CD105, at a ratio of 1:500. The negative control was prepared by incubating only the secondary antibodies: Alexa Fluor 555 (Invitrogen) and Alexa Fluor 488 (Invitrogen). Cells were gently washed in the coverslip with PBS (4 times) to remove excessive antibodies, followed by fixation with PFA

4% for 2 h. Cells were gently washed again with PBS, and the coverslips fixed with Fluoromount (Sigma) onto a histological slide for further analysis. Images were acquired using an 8-bit gray scale confocal laser scanning microscope (Olympus FV1000). Approximately 10–15 sections with 0.7 µm thick confocal were captured parallel to the coverslip (XY sections) using a ×20 objective (Olympus, U plan-super-apochromat, UPLSAPO 60X). Z-stack reconstruction and analysis were conducted using ImageJ software (http://rsb.info.nih.gov/ij/).

2. Extracellular Vesicles (EVs)

2a. EVs isolation and purification

As cultured hAT-MSCs (P4-P8) reached 80% confluence, DMEM + 10% FBS medium was replaced by DMEM FBS-free (to avoid isolated vesicles contamination by FBS proteins). After 72 h of culture, the medium was collected for vesicles isolation and cells remained in culture. To recover from stress caused by FBS removal, the remained cells were supplemented with DMEM + 10% FBS for 72 h[29].

For EVs isolation, the medium was collected and centrifuged (3 times) at 4°C: (1st : 400×g for 15 min, 2nd : 2000×g for 15 min and 3rd : 10,000×g for 30 min). The supernatants were filtered through a 0.22 µm membrane. The isolation was finished by centrifugation (100,000×g at 4°C for 2 h). The supernatant was discarded, PBS was used to wash the pellet containing EVs, and the cell suspension was centrifuged at 100,000×g at 4°C for 2 h[41]. Finally, the pellet was resuspended in 100 µl of PBS and stored at −20°C[38]. EVs protein content was quantified by bicinchoninic acid (BCA) assay (Thermo Scientific Pierce™)[38]. The vesicles isolated from C0, C1 and C2 cells are named EV0, EV1 and EV2, respectively.

2b. EVs Characterization

EVs were characterized by flow cytometry and identification of membrane proteins CD63 and CD81 presence[42]. Firstly, EVs were incubated with magnetic beads (Thermo Fisher - Scientific - Invitrogen™) coated with primary antibody CD63 (Exosome-Human CD63, Thermo Fisher - Scientific - Invitrogen™) and CD81 (Exosome-Human CD81, Thermo Fisher - Scientific - Invitrogen™) for 18 h at 4°C under gentle stirring. For each preparation, 10 µl of 1 mg/ml EVs suspension was applied. To remove excess of beads, EVs were washed with PBS: 2mL of PBS was added for 5 minutes, then the tub was placed in a magnet for 1 minute and the supernatant was discarded. Then, CD63 (CD63 Anti-human Mouse, FITC, Clone: MEM-259, Invitrogen ™) and CD81 (PE Anti-Human Mouse CD81 Clone JS-81, BD Pharmingen ™) antibodies (without granules) were added to the solution containing the EVs + magnetic beads. After 1 h of incubation, the EVs were gently washed by placing the tube on a magnet for 1 minute, discarding the supernatant. We added 2mL of PBS (to remove excess antibody) for 5 minutes and again placed the tube on a magnet for 1 minute and discarded the supernatant. Finally, the EVs were resuspended in 200 µl of PBS for analysis. Ten thousand events were analyzed by flow cytometry.

To measure the particle size and the polydispersity index (PDI) we used photon correlation spectroscopy. The EVs suspension derived from hAT-MSCs (50 µl) at 1 mg/ml was diluted in 1 ml of PBS. All analyzes

were performed in triplicate using a Malvern Nano-ZS90® (Malvern Instruments, England) at 25 ° C.

2c. EVs Purity Measurement

Transmission electron microscopy (TEM) analysis, using direct examination technique, was used to evaluate EV purity and diameter sizes[37]. EVs suspension (10 µL), 1 mg/ml of protein, was aliquoted onto a grid covered with carbon film (formvar/carbon) and dried at room temperature. Uranyl was used as a contrast. The sample was analyzed by TEM 120Kv (JEM 1200 Exll-JEOL).

2d. EVs Labeling

EVs were labeled with red fluorescent membrane dye PKH26 (MINI26, Sigma). In brief, the EVs-containing PBS solution was centrifuged at 100,000×g for 2 h, at 4°C and the pellet suspended with the diluent of the fluorescent kit. Filtered PKH26 (4mM) and EVs (200 µg/ml) were mixed at a ratio 1:1 for 5 min, followed by the addition of 5% BSA. To remove excess dye, the EVs were washed (3 times): we added 5 ml of PBS and centrifuged at 100,000×g for 2 h, at 4°C, discarded the supernatant. In the last centrifugation, stained EVs pellet was suspended in 0.5 mL of PBS. To eliminate any dye aggregates, the solution was filtered through a 0.2 µm membrane filter [35].

3. Animals

3a. Characterization

Adults (90–120 days old) male Wistar rats weighting 350–400 g were maintained under controlled light (12/12 h light/dark cycle), 22°C ± 2, with water and food *ad libitum*.

All procedures were performed according to the Guide for the Care and Use of Laboratory Animals and to the Brazilian Society for Neuroscience and Behavior (SBNeC) recommendations for animal studies.
The Ethics Committee for the Use of Animals at the Universidade Federal do Rio Grande do Sul (process number: 31888) approved this project.
The schematic procedures are illustrated in Fig. 1.

3b. Focal Permanent Ischemia and Sham Procedures

Anesthetized animals (ketamine hydrochloride: 90 mg/kg, 450 µl/kg i.p. and xylazine hydrochloride:10 mg/kg, 300 µl/kg i.p.) were placed into a stereotaxic apparatus. After skin incision, the skull was exposed, and the craniotomy was performed by exposing the left frontoparietal cortex (+ 2mm to − 6mm A.P. and − 2mm to − 4mm M.L. from the bregma). A focal permanent ischemic lesion was induced by thermo-coagulation of motor and sensorimotor pial vessels [43–47]. Blood vessels were thermo-coagulated by placing a hot probe near the dura mater for 2 min, until red-brown color indicated complete thermo-coagulation. Soon after, the skin was sutured, and animals placed on a heating pad at 37°C, until full recovery from anesthesia. Animals from sham group were only submitted to the above-mentioned craniotomy. Animals were randomly allocated to 3 treatment groups: Sham; Ischemic (ISC); Ischemic treated with EVs (ISC + EV).

3c. Intranasal EVs Treatment

Intranasal EVs treatment was performed 24 h after ischemic or sham procedure. Sedated animals (O_2 flow rate at 0.8-1.0 L/min with Isoflurane levels of 2.5-3.0 %) slowly (during 20 sec) received, into the nasal cavity, a single 50 µL of EVs (ISC + EVs) or 50 µL PBS (Naive, Sham, ISC). The 200 µg/kg EVs dose was selected based on a dose/effect curve: ISC + PBS; ISC + 100 µg/kg; ISC + 200 µg/kg and ISC + 300 µg/kg (n = 3).

4. Brain analysis

4a. Extracellular Fluorescent Vesicles (EVs) Detection in Rat Brain

Distribution of EVs in rat brains was analyzed 18 h after intranasal administration of fluorescent EVs (PKH26-mini, Sigma)[32, 35, 37]. Anesthetized animals (ketamine hydrochloride: 90 mg/kg, 450 µl/kg i.p. and xylazine hydrochloride: 10 mg/kg, 300 µl/kg i.p.) were transcardially perfused using a peristaltic pump with PBS followed by perfusion with PFA 4% (both 10 mL/min, 100mL). Brains were dissected and immersed in PFA 4%, pH 7.4 and stored for a maximum of 7 days at 4°C. Coronal brain Sect. 20 µm thick were obtained using a vibratome (Leica) at + 2.20 mm, 0,20 mm and − 1,88 mm of Bregma. Brain slices were mounted on glass slices and incubated for 5 min in the dark with 1 µg/mL Hoechst dye (33342 Sigma-Aldrich) in PBS to detect cell nuclei. The slices were washed with PBS (4 times) and the slices fixed with fluoro mount (Sigma).

Slices images for counting EVs were acquired using an 8-bit gray scale confocal laser scanning microscope (Olympus FV1000). Approximately 10–15 sections with 0.7 µm thick confocal were captured parallel to the coverslip (XY sections) using a ×60 objective (Olympus, U plan-super-apochromat, UPLSAPO 60X). Z-stack reconstruction and analysis to count the vesicles in the brain tissue were conducted using ImageJ software, briefly: background noise was removed using the “subtract background” tool. Images were converted to binary masks using default threshold option and vesicles were counted with the “analyze particles” tool (size = 0.05–0.90 µm). These settings were programmed into a macro and used for all analyzed images (http://rsb.info.nih.gov/ij/) (n = 3 naive and n = 5 ischemic for each group, 3 sections in each rat per group).

4b. Short term infarct volume

For the short-term evaluation of infarct volume, Naive, Sham, ISC, ISC + EV0 and ISC + EV2 groups were sedated 48 hours after treatment (O_2 flow rate of 0.8 -1.0 mL/min with Isoflurane levels of 2.5-3.0%) and culled. Coronal sections of the whole brains were sliced at 2 mm, immersed in 2% 2,3,5-Triphenyl-tetrazolium chloride (TTC). After 30 minutes of incubation at 37 ºC, the slices were dipped in 4% buffered paraformaldehyde (pH 7.4) for 24 hours. The size of the infarct area was evaluated as the area devoid red staining. Infarct volume was measured using the imageJ software[44] (3 rats/group, 6 sections/rat).

4c. Brain Angiogenesis

After 42 days of treatment, animals from groups Naive, ISC and ISC + EV2 were anesthetized and received intracardial injection of 50 mg/mL (500 µl) fluorescein isothiocyanate-dextran amine (Merck) to label brain blood vessels. Rat brains were removed, immediately fixed in PFA 4%, and cut at 30 µm coronal slices in a vibratome. Images were acquired in fluorescence microscope (Nikon). The images were taken from the ipsilateral and contralateral sides in the Secondary Motor Cortex (M2) and somatosensory regions (SS) using the coordinates: +2.20 mm, 0.2 mm and − 1.88 mm A.P. to Bregma (PAXINUS online Rat Brain Atlas: http://labs.gaidi.ca/rat-brain-atlas/) (n = 3 per group). Blood vessels parameters as the total length (sum of length of segments, isolated elements and branches in the analyzed area) and the number of branches (in the analyzed area) were quantified with the Angiogenesis Analyser Plugin (Gilles Carpentier Research) ImageJ software (https://imagej.nih.gov/ij/).

5. BBB permeability

5a. Evans Blue in brain parenchyma.

Naive (n = 3), Sham (n = 3), ISC (n = 3) and ISC + EV2 (n = 3) animals were anesthetized 48 hours after treatment (ketamine hydrochloride – 90 mg/kg, 450 µl/kg i.p. and xylazine hydrochloride 10 mg/kg, 300 µl/kg i.p.) and received 3 ml/kg of Evans Blue (EB) solution 2% in saline, through the gingival artery (Supplementary information 1). After 1 hour, the animals were submitted to cardiac perfusion using a peristaltic pump (10 mL/min, with PBS, 100mL). Animals were culled, their brains were removed, weighed and whole brain was sliced at 2 mm for image acquisition for each slice. After, all slices together from each brain were macerated and homogenized in 2.5 ml of PBS and vortexed for 2 minutes. For the precipitation of proteins, 2.5 ml of 50% trichloroacetic acid was added to the homogenate, incubated for 12 hours at 50 ºC, centrifuged at 14,000 x g for 10 minutes. The concentration of the blue color was measured by a spectrophotometer (620 nm). EB dye was expressed in µg/g brain tissue against a standard curve [48, 49].

5b. CSF albumin levels

Albumin assay was performed using High Performance Liquid Chromatography coupled to Fluorescence detector (HPLC-FLD). The CSF method was validated according with the FDA guidelines [50, 51]. HPLC-FLD consisting of LC Shimadzu system (Kyoto, Japan) equipped with LC- 20AT pump, DGU-14A degasser, thermostat for CTO-10A column and Fluorescence detector, RF 20A was used. Acquisition and processing of the data was obtained using the LC Solution software. The FLD was set at 278 nm (excitation) and 335 nm (emission). Agilent reversed-phase ZORBAX SB-C18 column (5 µm particle size, 250 × 4.6 mm i.d.) was used. The method was performed using gradient condition, consisting of solvent A (H_2O + 0.1% formic acid) and solvent B (acetonitrile (ACN) as follows: A → 65% B → 35% (0–5 min), A → 70% B → 30% (5–10 min), A → 65% B → 35% (10–17 min). The flow rate was set at 0.7 mL/min. Samples preparation was performed by adding to a 10 µL liquor in 40 µL of ACN and mixed in a vortex. The solution was transferred to conical vials and 10 µL was injected. Albumin stock solutions 1 mg/mL in water were stored at − 20 ± 2°C. For each day of analysis, standard solutions of albumin were prepared at 0,1, 0,5, 1, 10, 50 and 100 µg/mL.

6. Behavioral evaluation

6a. Cylinder Task (CT)

The cylinder task, which allows the evaluation of motor sequelae caused by ischemic insult[52], were used to determine animal motor symmetry of front paws. Exploration of the apparatus by the rats was evaluated when they raised their bodies and contact their paw(s) on the cylinder wall (20 movements are counted). The apparatus consisted of a transparent glass cylinder 20 cm in diameter and 30 cm in height. All animals were submitted to this task 2 h before surgery, to verify the basal forelimb symmetry. The CT was repeated on the 3rd, 7th, 14th, 21st, 28th, 35th and 42nd days after EVs treatment. The performance was recorded using ANY-Maze software (Stoelting CO., Wood Dale, IL), and the ipsilateral (to the lesion), contralateral or both front paws preference were counted in a blind analysis. The asymmetry of each animal was calculated by the following formula: asymmetry = (% of ipsilateral paw use = Ipsilateral paw use / sum Ipsilateral + Contralateral + use of both paws) − (% of contralateral paw use = contralateral paw use / sum of Ipsilateral + Contralateral + use of both paws). The asymmetry percentage was converted into symmetry percentage[43]. Groups: Naive (n = 6), ISC (n = 22), ISC + EV0 (n = 17); ISC + EV1 (n = 16) and ISC + EV2 (n = 17). At the end of each task, the apparatus was cleaned using 70% ethanol solution.

6b. Open Field Task (OFT)

The open field task evaluates habituation to novelty (assessing short- and long-term memory - exploratory activity) and locomotor activity in an arena[53]. The apparatus consisted of a black cage measuring 50 cm in length × 50 cm in width × 50 cm in height. The sessions lasted 10 min (individually). Animals performed the task on the 7th, 21st and 42nd days after EVs treatment. Short-term memory (habituation to novelty) was evaluated considering the decrease of locomotion during the first 5 min of the 1st session (7th day). Long-term memory was evaluated considering the decrease in locomotion during the first minute through the successive sessions (from the 1st to the 3rd session). Groups: Naive (n = 8), Naïve + EV0 (n = 7), ISC (n = 22), ISC + EV0 (n = 17); ISC + EV1 (n = 16) and ISC + EV2 (n = 17). At the end of each session, the apparatus was cleaned with 70% ethanol solution. The task was recorded and analyzed using ANY-maze 6.1 software.

6c. Novel Object Recognition Task (NORT)

The behavioral sessions lasting 10 min were performed on the 7th, 21st and 42nd days after EVs treatment. 90 min after the OFT session, Object Recognition (OR) short- and long-term memories were evaluated[54]. Animals were individually placed on the periphery of the arena for exploration. Two identic familiar objects (FOs) were placed in the arena and animals were allowed to explore them for 10 min. Sniffing and touching the objects were considered as exploratory behavior. 90 min after the training session, each animal was placed back into the arena to evaluate short-term memory. One of the 2 FOs used in the training session was replaced by a new distinct object (NO). The long-term memory was evaluated 24 h after the short-term memory task session, when the animals were placed back in the arena

with same FO used in the training session and in first test session (short-term memory), while the same NO was displaced to a different position. In all sessions, the time spent exploring the objects was recorded by using ANY-maze 6.1 software. Results were expressed as a percentage of time exploring each object. Animals that recognized the novel object (short-term memory) or its new position (long-term memory), explored it more than 50% of the total exploring time of both objects. Groups: Naive (n = 8), Naive + EV0 (n = 7), ISC (n = 22), ISC + EV0 (n = 17); ISC + EV1 (n = 5) and ISC + EV2 (n = 16). At the end of each session, the apparatus was cleaned using 70% ethanol solution.

6d. Elevated Plus-maze Task (EPMT)

The EPMT task is widely used to study anxiety-like behavior[55]. The apparatus had 2 open arms (50 cm long × 10 cm wide) and 2 closed arms (50 cm long × 10 cm wide × 40 cm high), separated by a central platform (5 cm long × 5 cm wide). The apparatus was placed 70 cm high from the floor. The animals were kept in a red-light area for 1 hour before starting this task. ANY-maze software was used to record behavioral performance for 5 min. The percentage of time spent in open and closed arms was assessed. Anxiety-like behavior was considered as the increase of time spent on closed arms. Each animal conducted this once, on the 7th day after treatment with EVs. At the end of each session, the equipment was cleaned with 70% alcohol.

7. Statistical Analysis

The size of the brain lesion, BBB integrity, number of vesicles found in brain tissue and angiogenesis analysis were evaluated by unpaired T-tests. Two-way RM ANOVA was applied for CT, followed by Sidak's multiple comparisons test. Short-term memory was evaluated by unpaired t-test. Long-term memory was evaluated by two-way ANOVA followed by Sidak's multiple comparisons test. Unpaired T-tests were used for the NORT with a theoretical average of 50%. Data are reported as the mean ± SD. All analyses were performed using Graph Pad Prism 6.0.

Results

1. hAT-MSCs and EVs

1a. hAT-MSCs Characterization

Figure 2. There is no single marker to characterize hADSCs, which is done by immunophenotyping based on the presence (> 70%) of CD90 and CD105, associated with the absence (< 5%) of CD34 and CD45[29]. Displacement of the fluorescence peaking to the right side registers a positive value for protein markers presence. More than 70% of C1, C2 and C3 cells were positive for CD90 and CD105, while only 0.3% of the analyzed cells were positive for CD45 and CD34, which is a characteristic of these cells. The cells were also characterized by fluorescence microscopy with the same markers.

1b. Extracellular Vesicles (EVs) Characterization,

Figure 3. EVs were detected inside the C0 cells by confocal microscopy through the presence of CD63 and CD81 marking (Fig. 3a, 3b and 3c). They were detected in the plasma membrane and in the cytoplasm near to the nucleus. The released EVs (EV0, EV1 and EV2) were analyzed by measuring CD63 and CD81 marking through flow cytometry; more than 90% of the EVs presented CD63 and CD81[42] (Fig. 2d). The released EVs (EV0, EV1 and EV2), were also analyzed by Zetasizer instrument, which indicated the average diameter of 140 nm, with a polydispersity index (PDI) average of 0.3 (Fig. 3e). The purity of released EVs suspension was confirmed by the TEM-direct technique. The suspension only consisted of released vesicles with cylindrical morphology and electron dense membranes (indicated by the black arrow in Fig. 3f).

2. Stroke damage and EVs neuroprotection

2a. EVs administration on motor neuroprotection

- Dose curve of EV1 administration and motor neuroprotection

Figure 4. The cylinder task (CT) measures front paw symmetry and was applied to identify the lowest dose to be used for EV stroke treatment. All animals underwent the CT task 24 h before stroke (day − 1). Of note, only animals presenting ~ 100% front paw symmetry were included in the study. Further, we performed intranasal administration of EV0 or vehicle 24h after stroke. Indeed, 72 h after stroke, all ISC groups, treated or not, presented a mean symmetry of 30%. Interestingly, animals treated with EVs showed gradual improvement in symmetry of the front paws compared to untreated animals in a time and dose dependent manner: at the 42nd day after intranasal administration, animals in the vehicle and treated EVs (100µg/kg, 200µg/kg or 300µg/kg) groups presented symmetry recovery of 58% ±6, 67% ±4%, 87% ±8 and 82% ±3, respectively. Animals receiving 200µg/kg or 300 µg/kg did not differ from naive group from the 21st day after treatment with VES (95% ±3), suggesting a total recovery of symmetry. In keeping with this, the dose of 200 µg/kg at 24 h after stroke was selected for the further experiments.

• Effect of 200µg/kg treatment of EVs on neuromotor recovery

Figure 5. EV0, EV1 and EV2 treatments, applied 24h after stroke, caused a time dependent recovery of front paw symmetry from the 7th day after treatment (ISC: 31%±11, ISC + EV0: 63%±15, ISC + EV1: 67% ±13, ISC + EV2: 66%±13 symmetry, $p < 0.0001$), reaching total recovery until the 28th day (ISC: 43%±14, ISC + EV0: 82%±9, ISC + EV1: 76%±9, ISC + EV2: 82%±6 symmetry, $p < 0.0001$). On the 42nd day (last evaluation) ISC + EVs groups had similar symmetry to naive group (Naive: 95%±02, ISC + EV0: 86%±10, ISC + EV1: 86%±05, ISC + EV2: 80%±05 symmetry).

2b. Short term infarct volume

Figure 6. The infarct volume was evaluated 72 hours after the ischemic insult (48 hours after treatment). Treatment with 200 µg/kg EVs significantly decreased the volume of infarct (ISC x ISC + EV0 $p < 0.05$, ISC x ISC + EV2, $p < 0.05$).

2c. *BBB permeability*

As illustrated in Fig. 7, stroke affected the BBB permeability, an effect partially attenuated by EVs treatment. These findings were demonstrated by Evans blue dye penetration into brain parenchyma (Fig. 7a and 7b) and by an increase of CSF albumin levels (Fig. 7c) (ISC x ISC + EV3, $p < 0.05$).

2d. Extracellular Vesicles Detection (EVs) in Rat Brain

Figure 8. The distribution of EV0 (200 µg/kg) in the cortical brain was evaluated. The images were acquired in the position 2.2mm, 0.2mm and − 1.88mm A.P. of Bregma (Fig. 8a). The regions were: 2 ipsilateral peri-infarct regions and their contralateral equivalents, specifically Supplementary Motor Cortex (M2) and somatosensory regions (SS). Remarkably, there was no homogeneous distribution of EVs. In the ISC group, the M2-ipsilateral (M2-I) and M2-contralateral (M2-C) regions had a greater number of vesicles compared to the naive animals and to the ISC SS-ipsilateral (SS-I), ISC SS-Contralateral (SS-C) (Fig. 8b; $p < 0.0001$). Figure 4C-H show representative images of these findings.

2e. Open Field Task (OFT)

Figure 9. This task evaluates the habituation to novelty. Animals were submitted to 3 sequential OFT sessions: in the 7th, 21st and 42nd days after EVs treatment. All groups presented short-term memory (evaluated only in the 1st exhibition). Naive groups also presented long-term memory, which was impaired by stroke; EV0, EV1 and EV2 treatment abolished this effect.

2f. Novel Object Recognition Task (NORT)

Figure 10. The NORT was used to evaluate short- and long-term memory of object recognition (OR) on the 7th, 21st and 42nd days after EV0, EV1 or EV2 treatment. Stroke impaired both short- and long-term memory, an effect abolished by EVs treatment.

2g. Elevated Plus-maze Task (EPMT)

Figure 11. The elevated plus-maze task is widely used to evaluate anxiety-like behavior. The task was performed on the 7th day after treatment with EVs. ISC animals spent more time on the closed arms compared to other groups, indicating that stroke induced an anxiogenic-like effect. Interestingly, the anxiety like behavior due to stroke was completely abolished by EV0 and EV1 treatment.

2h. Brain angiogenesis

Figure 12. Stroke decreased the number of branches and the total length of blood vessels in the cortical M2-I region, (Fig. 12b and 12c). The reduction on the number of branches was abolished by EVs treatment. Figures 12d-12i show representative images of the M2 regions. In SS regions, there was no difference among all groups (Supplementary information 2).

Discussion

The two available strategies for stroke treatment are the use of thrombolytic agents and the mechanical removal of the thrombus. Nevertheless, in both cases accessibility may be limited. In fact, thrombolytic agents have to be strictly applied within 4.5 h after the first symptoms [15], while specialized equipment and highly trained people are required to remove the thrombus [19]. In keeping with this, the search for innovative and more accessible treatment strategies for stroke are extremely relevant.

In this work, we demonstrated for the first time that the use of intranasal hAT-MSC-derived EVs offers a broader early intervention opportunity (24 hours after the stroke), pointing to a potentially valuable stroke treatment strategy. Although there are studies showing neuroprotective effects of MSC-derived EVs on stroke [30, 32, 34], most of them apply systemic administration, a protocol in which EVs are detected in other organs than the brain, as lungs, liver and spleen [32, 33], where they may be metabolized before reaching the cerebral parenchyma [56]. In these studies, the EVs were identified in brain regions but no study compared the number of EVs among regions [37, 56, 57] thus the EVs tropism for specific brain regions was not previously reported.

Indeed, our findings demonstrated a non-homogenous distribution in the ischemic group: ipsi- and contra-lateral M2 peri-infarct regions contained more EVs, compared to the SS regions (and also compared to the M2 and SS regions of naïve animals), indicating a higher EVs tropism to peri-infarct region. These results are in accordance with various previous works, which have focused on stroke treatment strategies targeting the peri-infarct region, aiming to stimulate angiogenesis [58, 59] and to modulate the BBB permeability [33, 59].

Clinical data from stroke patients have shown that behavioral and motor impairment are dependent on the regions of the brain where the infarct core and the penumbra zone are developed [3]. Accordingly, our and other research groups have already shown that in the ischemic stroke rat model here used, the core and peri-infarct regions are located in the prefrontal cortex and hippocampus [43–47], brain structures involved in neuromotor and memory modulation [60, 61]. Here, our stroke model caused a localized BBB impairment (acutely measured by Evans blue) and a decrease in the vascularization (chronically measured), both specifically in peri-infarct regions. Interestingly, a higher EVs tropism was observed to the same peri-infarct regions where a BBB recovery and vascularization improvement were demonstrated. This association points to a potential role of hAT-MSC derived EVs in brain located tissue repair, thus promoting motor and behavioral recovery.

In fact, stimulation of angiogenesis has been show to improve neurologic and motor function in animal stroke models [62, 63], an effect currently acknowledged as outcome of EVs transfer of protein, mRNA

and miRNA to endothelial cells [64], regulating proteins expression [65]. The BBB impairment in ischemic stroke is also documented [66], but its involvement in EVs therapeutic strategies was not previously reported.

We believe that our work shed light into a new and straightforward therapeutic strategy for focal permanent stroke treatment, by utilizing hAT-MSCs from healthy individuals as a source for EVs. In addition, the intranasal hAT-MSCs-derived EVs administration 24 h after brain injury induced a long-term neuroprotective effect, offering a remarkable broader therapeutic time window, compared to current standard systemic routes. Together, these findings point to a potential therapeutic strategy for patients with focal permanent ischemic stroke.

Declarations

Funding

The authors disclosed receipt of the following financial support for the research, authorship, and/or publication of this article: This study is funded by Instituto Nacional de Ciência e Tecnologia – INCT-EN (2014 - 465671/2014-4), Conselho Nacional de Desenvolvimento Científico e Tecnológico - CNPq, Ministério da Saúde, Coordenação de Aperfeiçoamento de pessoal de Nível Superior - CAPES, Fundação de Amparo à pesquisa do Estado do Rio Grande do Sul - FAPERGS, Universidade Federal do Rio Grande do Sul - UFRGS

Declaration of conflicting interests

The authors declared no potential conflicts of interest with respect to the research, authorship, and/or publication of this article.

Availability of data and material

The authors assume the availability of data and materials

Author contributions

All authors contributed in all stages of this work, read and approved the final manuscript.

Compliance with ethical standards

The study was performed in accordance with the ethical standards as laid down in the 1964 Declaration of Helsinki and its later amendments or comparable ethical standards. All procedures with animals were performed according to the Guide for the Care and Use of Laboratory Animals and to the Brazilian Society for Neuroscience and Behavior (SBNeC) recommendations for animal studies. The Ethics Committee for the Use of Animals at the Universidade Federal do Rio Grande do Sul (process number: 31888) approved this project. The animals were followed up after the surgery, if signs of pain, discomfort, inflammation,

and any other symptoms that indicate the animal's suffering were observed, after the surgery, it was euthanized, thus avoiding its suffering (Humanitarian endpoint).

Consent to participate

All participants who donated adipose tissue for cell isolation signed a free and informed consent form as recommended and approved by the Research and Graduate Group (Grupo de Pesquisa e Pós-Graduação: GPPG 2018-0374) and Research Ethics Committee (Comite de Ética em Pesquisa CAEE -: 94521618.4.0000.5327) of the Experimental Research Center at Hospital de Clínicas de Porto Alegre.

This document described the entire objective of the research and that these data could be published in a scientific journal maintaining the confidentiality of the participants' personal data (anonymous donation)

Consent for Publication: Not applicable.

Acknowledgments: Not applicable.

References

1. World Health Organization (2018) WHO - The top 10 causes of death. In: 24 Maggio. http://www.who.int/en/news-room/fact-sheets/detail/the-top-10-causes-of-death
2. Tarver T (2014) Heart Disease and Stroke Statistics–2014 Update: a Report From the American Heart Association
3. Powers WJ, Rabinstein AA, Ackerson T, et al (2019) Guidelines for the early management of patients with acute ischemic stroke: 2019 update to the 2018 guidelines for the early management of acute ischemic stroke a guideline for healthcare professionals from the American Heart Association/American Stroke A
4. Surawan J, Sirithanawutichai T, Areemit S, et al (2018) Prevalence and factors associated with memory disturbance and dementia after acute ischemic stroke. Neurol Int 10:83–89. https://doi.org/10.4081/ni.2018.7761
5. Mitchell AJ, Sheth B, Gill J, et al (2017) Prevalence and predictors of post-stroke mood disorders: A meta-analysis and meta-regression of depression, anxiety and adjustment disorder. Gen Hosp Psychiatry 47:48–60. https://doi.org/10.1016/j.genhosppsych.2017.04.001
6. Tan HH, Xu J, Teoh HL, et al (2017) Decline in changing montreal cognitive assessment (MoCA) scores is associated withpost-stroke cognitive decline determined by a formal neuropsychological evaluation. PLoS One 12:3–6. https://doi.org/10.1371/journal.pone.0173291
7. Tomašević Todorović S, Kopčanski S, Mikov A, et al (2015) Functional Status of Patients After Stroke. Med Pregl 68:181–186. https://doi.org/10.2298/MPNS1506181T
8. Hatem SM, Saussez G, della Faille M, et al (2016) Rehabilitation of motor function after stroke: A multiple systematic review focused on techniques to stimulate upper extremity recovery. Front Hum Neurosci 10:1–22. https://doi.org/10.3389/fnhum.2016.00442

9. Akyurekli C, Le Y, Richardson RB, et al (2015) A Systematic Review of Preclinical Studies on the Therapeutic Potential of Mesenchymal Stromal Cell-Derived Microvesicles. Stem Cell Rev Reports 11:150–160. https://doi.org/10.1007/s12015-014-9545-9
10. Mellon L, Brewer L, Hall P, et al (2015) Cognitive impairment six months after ischaemic stroke: A profile from the ASPIRE-S study. BMC Neurol 15:1–9. https://doi.org/10.1186/s12883-015-0288-2
11. Donnan GA, Baron JC, Ma H, Davis SM (2009) Penumbral selection of patients for trials of acute stroke therapy. Lancet Neurol 8:261–269. https://doi.org/10.1016/S1474-4422(09)70041-9
12. Ren C, Yao Y, Han R, et al (2018) Cerebral ischemia induces angiogenesis in the peri-infarct regions via Notch1 signaling activation. Exp Neurol 304:30–40. https://doi.org/10.1016/j.expneurol.2018.02.013
13. Lo EH (2008) A new penumbra: Transitioning from injury into repair after stroke. Nat Med 14:497–500. https://doi.org/10.1038/nm1735
14. Uzdensky AB (2019) Apoptosis regulation in the penumbra after ischemic stroke: expression of pro- and antiapoptotic proteins. Apoptosis 24:687–702. https://doi.org/10.1007/s10495-019-01556-6
15. Baron JC (2018) Protecting the ischaemic penumbra as an adjunct to thrombectomy for acute stroke. Nat Rev Neurol 14:325–337. https://doi.org/10.1038/s41582-018-0002-2
16. Rabinstein AA (2017) Tratamiento Agudo De Evc Isquemico. Continuum (N Y) 62–81
17. Fonarow GC, Smith EE, Saver JL, et al (2011) Timeliness of tissue-type plasminogen activator therapy in acute ischemic stroke: Patient characteristics, hospital factors, and outcomes associated with door-to-needle times within 60 minutes. Circulation 123:750–758. https://doi.org/10.1161/CIRCULATIONAHA.110.974675
18. Anttila JE, Whitaker KW, Wires ES, et al (2017) Role of microglia in ischemic focal stroke and recovery: focus on Toll-like receptors. Prog Neuro-Psychopharmacology Biol Psychiatry 79:3–14. https://doi.org/10.1016/j.pnpbp.2016.07.003
19. Wang X, Tsuji K, Lee SR, et al (2004) Mechanisms of hemorrhagic transformation after tissue plasminogen activator reperfusion therapy for ischemic stroke. Stroke 35:2726–2730. https://doi.org/10.1161/01.STR.0000143219.16695.af
20. Brinjikji W, Rabinstein AA, McDonald JS, Cloft HJ (2014) Socioeconomic disparities in the utilization of mechanical thrombectomy for acute ischemic stroke in US hospitals. Am J Neuroradiol 35:553–556. https://doi.org/10.3174/ajnr.A3708
21. Nogueira RG, Jadhav AP, Haussen DC, et al (2018) Thrombectomy 6 to 24 Hours after Stroke with a Mismatch between Deficit and Infarct. N Engl J Med 378:11–21. https://doi.org/10.1056/nejmoa1706442
22. Hosseini SM, Farahmandnia M, Razi Z, et al (2015) 12 Hours After Cerebral Ischemia Is the Optimal Time for Bone Marrow Mesenchymal Stem Cell Transplantation. Neural Regen Res 10:904–908. https://doi.org/10.4103/1673-5374.158354
23. Xu Y, Du SW, Yu XG, et al (2014) Human bone marrow mesenchymal stem cell transplantation attenuates axonal injury in stroke rats. Neural Regen Res 9:2053–2058.

https://doi.org/10.4103/1673-5374.147930

24. Gómez-De Frutos MC, Laso-Garciá F, Diekhorst L, et al (2019) Intravenous delivery of adipose tissue-derived mesenchymal stem cells improves brain repair in hyperglycemic stroke rats. Stem Cell Res Ther 10:1–13. https://doi.org/10.1186/s13287-019-1322-x
25. Ridge SM, Sullivan FJ, Glynn SA (2017) Mesenchymal stem cells: Key players in cancer progression. Mol Cancer 16:1–10. https://doi.org/10.1186/s12943-017-0597-8
26. Camussi G, Deregibus MC, Bruno S, et al (2010) Exosomes/microvesicles as a mechanism of cell-to-cell communication. Kidney Int 78:838–848. https://doi.org/10.1038/ki.2010.278
27. Chen CC, Liu L, Ma F, et al (2016) Elucidation of Exosome Migration Across the Blood–Brain Barrier Model In Vitro. Cell Mol Bioeng 9:509–529. https://doi.org/10.1007/s12195-016-0458-3
28. Chen J, Chopp M (2018) Exosome therapy for stroke. Stroke 49:1083–1090. https://doi.org/10.1161/STROKEAHA.117.018292
29. Ni H, Yang S, Siaw-Debrah F, et al (2019) Exosomes derived from bone mesenchymal stem cells ameliorate early inflammatory responses following traumatic brain injury. Front Neurosci 13:1–10. https://doi.org/10.3389/fnins.2019.00014
30. Han Y, Seyfried D, Meng Y, et al (2019) Multipotent mesenchymal stromal cell-derived exosomes improve functional recovery after experimental intracerebral hemorrhage in the rat. J Neurosurg 131:290–300. https://doi.org/10.3171/2018.2.JNS171475
31. Williams AM, Dennahy IS, Bhatti UF, et al (2019) Mesenchymal Stem Cell-Derived Exosomes Provide Neuroprotection and Improve Long-Term Neurologic Outcomes in a Swine Model of Traumatic Brain Injury and Hemorrhagic Shock. J Neurotrauma 36:54–60. https://doi.org/10.1089/neu.2018.5711
32. Otero-Ortega L, Laso-García F, Del Carmen Gómez-De Frutos M, et al (2017) White matter repair after extracellular vesicles administration in an experimental animal model of subcortical stroke. Sci Rep 7:1–11. https://doi.org/10.1038/srep44433
33. Yang J, Zhang X, Chen X, et al (2017) Exosome Mediated Delivery of miR-124 Promotes Neurogenesis after Ischemia. Mol Ther - Nucleic Acids 7:278–287. https://doi.org/10.1016/j.omtn.2017.04.010
34. Otero-Ortega L, Gómez de Frutos MC, Laso-García F, et al (2018) Exosomes promote restoration after an experimental animal model of intracerebral hemorrhage. J Cereb Blood Flow Metab 38:767–779. https://doi.org/10.1177/0271678X17708917
35. Longa Q, Upadhya D, Hattiangady B, et al (2017) Intranasal MSC-derived A1-exosomes ease inflammation, and prevent abnormal neurogenesis and memory dysfunction after status epilepticus. Proc Natl Acad Sci U S A 114:E3536–E3545. https://doi.org/10.1073/pnas.1703920114
36. Kodali M, Castro OW, Kim DK, et al (2020) Intranasally administered human msc-derived extracellular vesicles pervasively incorporate into neurons and microglia in both intact and status epilepticus injured forebrain. Int J Mol Sci 21:. https://doi.org/10.3390/ijms21010181
37. Perets N, Betzer O, Shapira R, et al (2019) Golden Exosomes Selectively Target Brain Pathologies in Neurodegenerative and Neurodevelopmental Disorders. Nano Lett 19:3422–3431.

https://doi.org/10.1021/acs.nanolett.8b04148

38. Ohta Y, Takenaga M, Hamaguchi A, et al (2018) Isolation of adipose-derived stem/stromal cells from cryopreserved fat tissue and transplantation into rats with spinal cord injury. Int J Mol Sci 19:. https://doi.org/10.3390/ijms19071963
39. Nalamolu KR, Venkatesh I, Mohandass A, et al (2019) Exosomes treatment mitigates ischemic brain damage but does not improve post-stroke neurological outcome. Cell Physiol Biochem 52:1280–1291. https://doi.org/10.33594/000000090
40. Trinh NT, Yamashita T, Tu TC, et al (2016) Microvesicles enhance the mobility of human diabetic adipose tissue-derived mesenchymal stem cells in vitro and improve wound healing in vivo. Biochem Biophys Res Commun 473:1111–1118. https://doi.org/10.1016/j.bbrc.2016.04.025
41. Scholl JN, De Fraga Dias A, Pizzato PR, et al (2020) Characterization and antiproliferative activity of glioma-derived extracellular vesicles. Nanomedicine 15:1001–1018. https://doi.org/10.2217/nnm-2019-0431
42. Gurunathan S, Kang M-H, Jeyaraj M, et al (2019) Review of the Isolation, Characterization, Biological Function, and Multifarious Therapeutic Approaches of Exosomes. Cells 8:307. https://doi.org/10.3390/cells8040307
43. de Vasconcelos dos Santos A, da Costa Reis J, Diaz Paredes B, et al (2010) Therapeutic window for treatment of cortical ischemia with bone marrow-derived cells in rats. Brain Res 1306:149–158. https://doi.org/10.1016/j.brainres.2009.09.094
44. Teixeira LV, Almeida RF, Rohden F, et al (2018) Neuroprotective Effects of Guanosine Administration on In Vivo Cortical Focal Ischemia in Female and Male Wistar Rats. Neurochem Res 43:1476–1489. https://doi.org/10.1007/s11064-018-2562-3
45. Nonose Y, Gewehr PE, Almeida RF, et al (2018) Cortical Bilateral Adaptations in Rats Submitted to Focal Cerebral Ischemia: Emphasis on Glial Metabolism. Mol Neurobiol 55:2025–2041. https://doi.org/10.1007/s12035-017-0458-x
46. Hansel G, Tonon AC, Guella FL, et al (2015) Guanosine Protects Against Cortical Focal Ischemia. Involvement of Inflammatory Response. Mol Neurobiol 52:1791–1803. https://doi.org/10.1007/s12035-014-8978-0
47. Hansel G, Ramos DB, Delgado CA, et al (2014) The potential therapeutic effect of guanosine after cortical focal ischemia in rats. PLoS One 9:1–10. https://doi.org/10.1371/journal.pone.0090693
48. Wang HL, Lai TW (2014) Optimization of Evans blue quantitation in limited rat tissue samples. Sci Rep 4:1–7. https://doi.org/10.1038/srep06588
49. Dal-Pizzol F, Rojas HA, Dos Santos EM, et al (2013) Matrix metalloproteinase-2 and metalloproteinase-9 activities are associated with blood-brain barrier dysfunction in an animal model of severe sepsis. Mol Neurobiol 48:62–70. https://doi.org/10.1007/s12035-013-8433-7
50. European medicines agency. (2012) Guideline on bioanalytical method validation guideline on bioanalytical method validation
51. FDA (2018) Guidance for industry: bioanalytical method validation. 1–44

52. MacRae I (2011) Preclinical stroke research - Advantages and disadvantages of the most common rodent models of focal ischaemia. Br J Pharmacol 164:1062–1078. https://doi.org/10.1111/j.1476-5381.2011.01398.x
53. Almeida RF de, Ganzella M, Machado DG, et al (2017) Olfactory bulbectomy in mice triggers transient and long-lasting behavioral impairments and biochemical hippocampal disturbances. Prog Neuro-Psychopharmacology Biol Psychiatry 76:1–11. https://doi.org/10.1016/j.pnpbp.2017.02.013
54. Figueiredo CP, Clarke JR, Ledo JH, et al (2013) Memantine rescues transient cognitive impairment caused by high-molecular-weight Aβ oligomers but not the persistent impairment induced by low-molecular-weight oligomers. J Neurosci 33:9626–9634. https://doi.org/10.1523/JNEUROSCI.0482-13.2013
55. Almeida RF, Cereser VH, Faraco RB, et al (2010) Systemic administration of GMP induces anxiolytic-like behavior in rats. Pharmacol Biochem Behav 96:306–311. https://doi.org/10.1016/j.pbb.2010.05.022
56. Dabrowska S, Andrzejewska A, Strzemecki D, et al (2019) Human bone marrow mesenchymal stem cell-derived extracellular vesicles attenuate neuroinflammation evoked by focal brain injury in rats. J Neuroinflammation 16:1–15. https://doi.org/10.1186/s12974-019-1602-5
57. András IE, Toborek M (2016) Extracellular vesicles of the blood-brain barrier. Tissue Barriers 4:1–6. https://doi.org/10.1080/21688370.2015.1131804
58. Cirillo C, Brihmat N, Castel-Lacanal E, et al (2020) Post-stroke remodeling processes in animal models and humans. J Cereb Blood Flow Metab 40:3–22. https://doi.org/10.1177/0271678X19882788
59. Rust R (2020) Insights into the dual role of angiogenesis following stroke. J Cereb Blood Flow Metab 40:1167–1171. https://doi.org/10.1177/0271678X20906815
60. Morici JF, Bekinschtein P, Weisstaub N V. (2015) Medial prefrontal cortex role in recognition memory in rodents. Behav Brain Res 292:241–251. https://doi.org/10.1016/j.bbr.2015.06.030
61. Zhou LYY, Wright TE, Clarkson AN (2016) Prefrontal cortex stroke induces delayed impairment in spatial memory. Behav Brain Res 296:373–378. https://doi.org/10.1016/j.bbr.2015.08.022
62. Slevin M, Kumar P, Gaffney J, et al (2006) Can angiogenesis be exploited to improve stroke outcome? Mechanisms and therapeutic potential. Clin Sci 111:171–183. https://doi.org/10.1042/CS20060049
63. Kanazawa M, Takahashi T, Ishikawa M, et al (2019) Angiogenesis in the ischemic core: A potential treatment target? J Cereb Blood Flow Metab 39:753–769. https://doi.org/10.1177/0271678X19834158
64. Todorova D, Simoncini S, Lacroix R, et al (2017) Extracellular vesicles in angiogenesis. Circ Res 120:1658–1673. https://doi.org/10.1161/CIRCRESAHA.117.309681
65. Gangadaran P, Rajendran RL, Lee HW, et al (2017) Extracellular vesicles from mesenchymal stem cells activates VEGF receptors and accelerates recovery of hindlimb ischemia. J Control Release 264:112–126. https://doi.org/10.1016/j.jconrel.2017.08.022

66. Yang C, Hawkins KE, Doré S, Candelario-Jalil E (2019) Neuroinflammatory mechanisms of blood-brain barrier damage in ischemic stroke. Am J Physiol - Cell Physiol 316:C135–C153. https://doi.org/10.1152/ajpcell.00136.2018

Figures

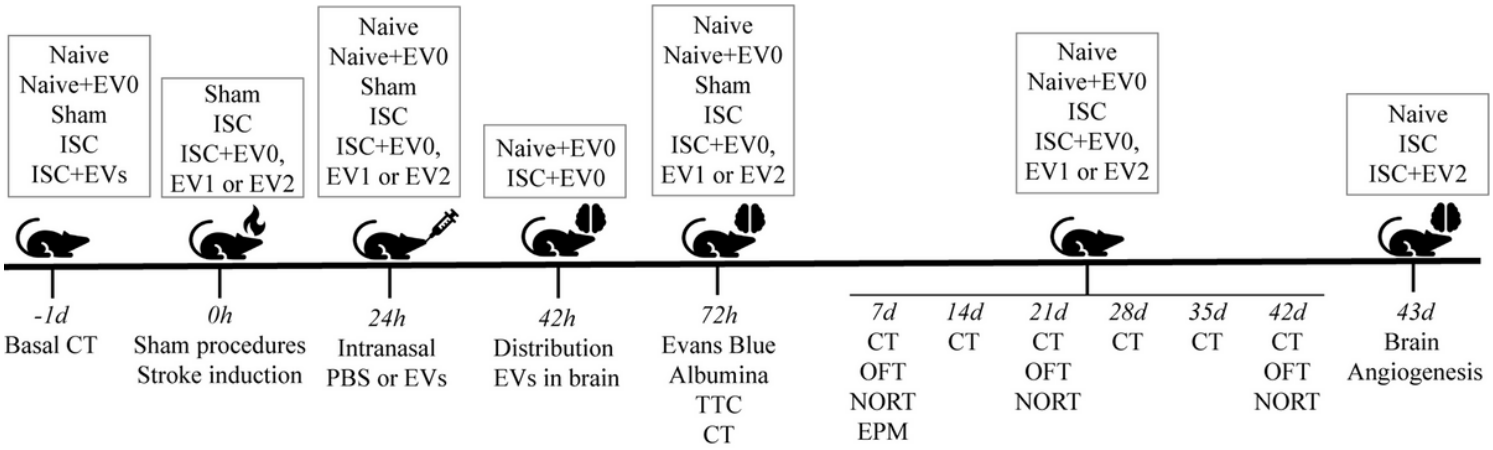

Figure 1

Experimental scheme. The animals received 50µl PBS or EVs by nostril 24hr after surgery. TTC: 2,3,5-Triphenyl-tetrazolium chloride; CT: Cylinder Task; OFT: Open Field Task; NORT: Novel Object Recognition Task. EPMT: Elevated Plus Maze Task; Naive: naive group; Sham: Sham group; ISC: ischemic group; ISC+EV0, EV1, EV2: ISC+Vesicles 1, 2, 3

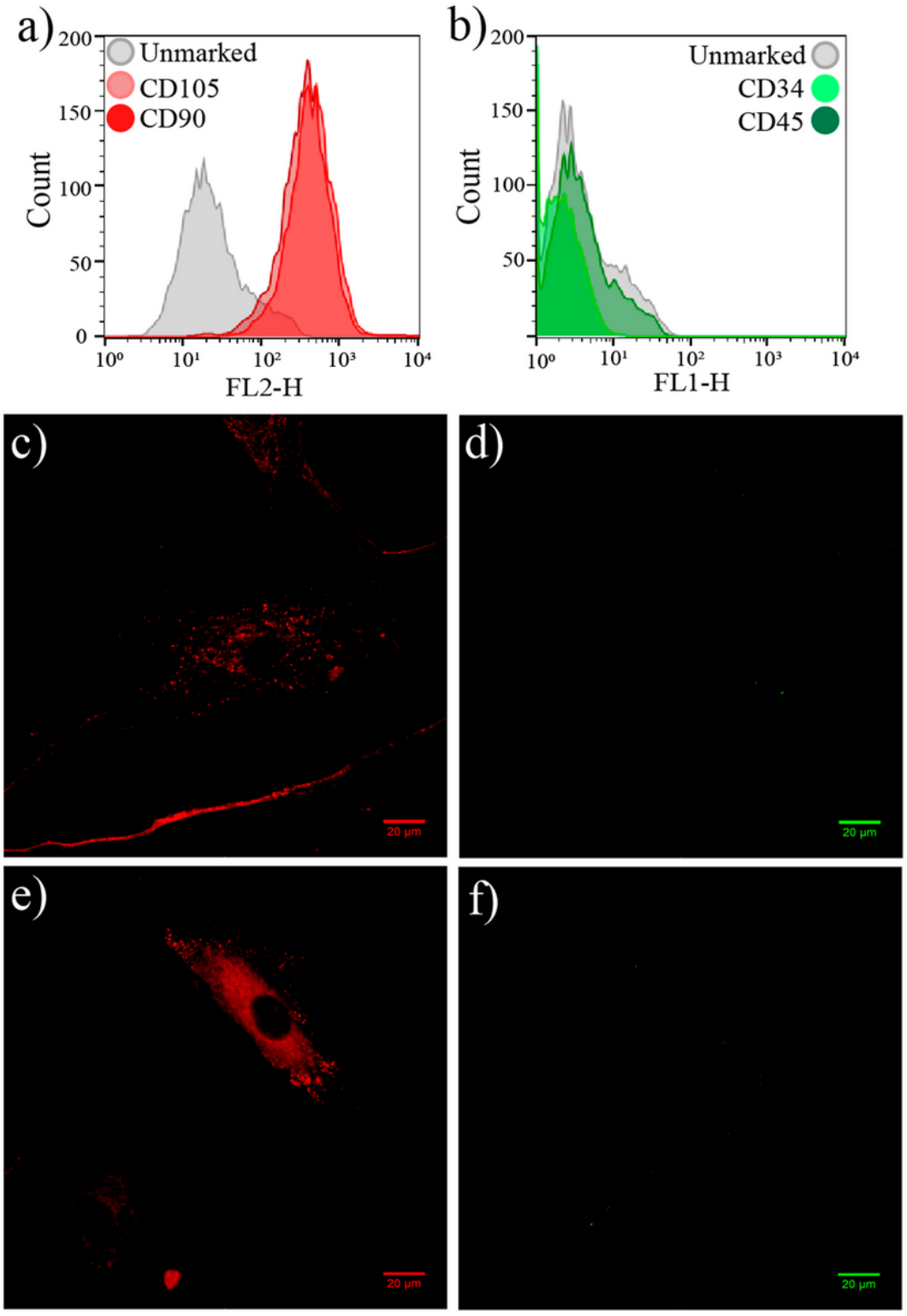

Figure 2

Representative images of cells by flow cytometry and fluorescence microscopy with CD labeling specific for hAT-MSCs. a) CD105 and CD90 (marking 70% of the cells). b) CD34 and CD45 (non-expression in both cells) c) to f) Representative images of cells from fluorescence microscopy, 40x objective: c) CD90 (red); d) CD45 (green); e) CD105 (red); f) CD34 (green). N=3, Scale bars: 20µm

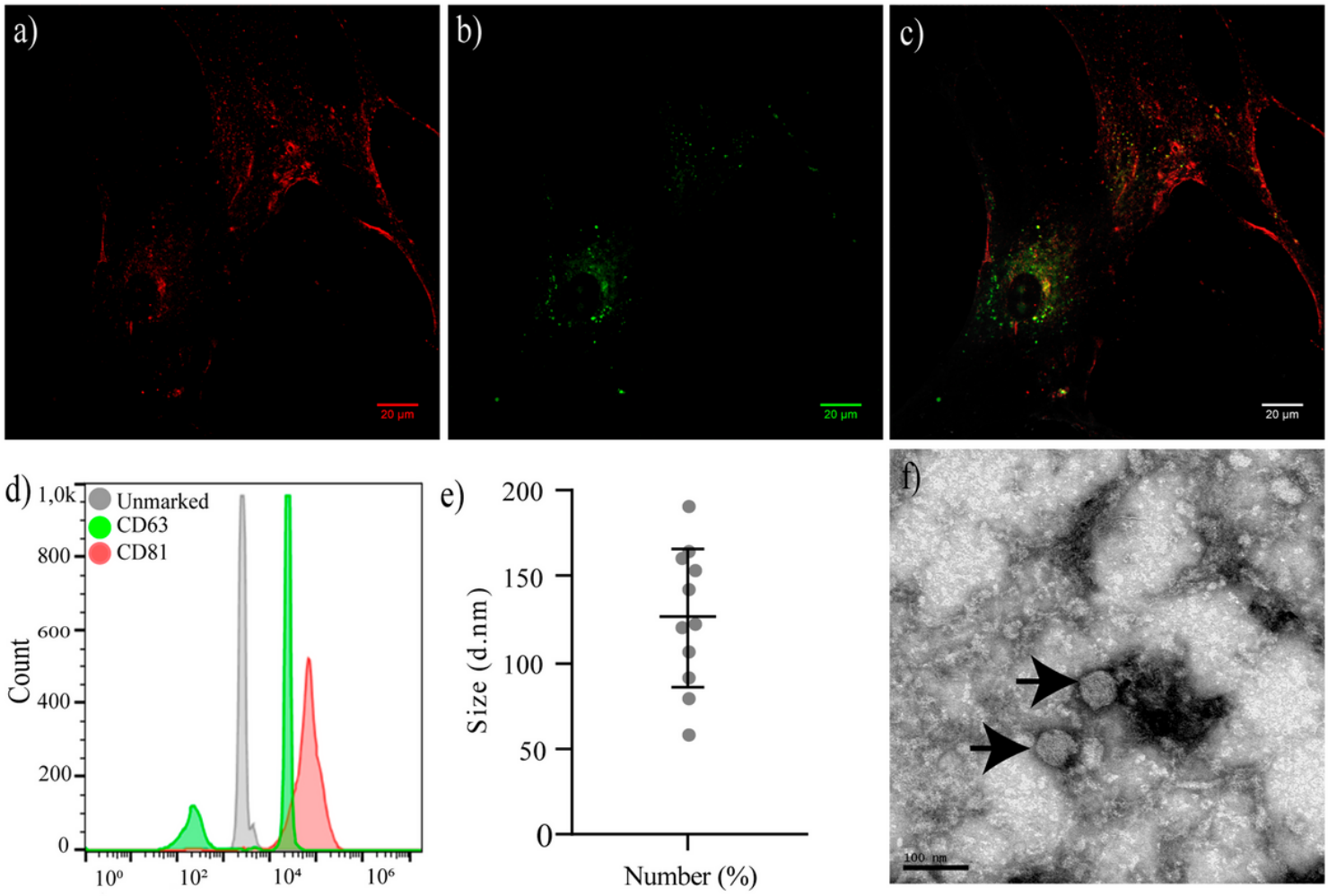

Figure 3

EVs Characterization. The fluorescence signals of following markers observed inside C0. a) CD81 (red), b) CD63 (green), c) Merge; N = 3. The fluorescence images were from a confocal microscope, using a 60x objective. Scale bars: 20 µm. d) Histogram of EVs characterization by flow cytometry with specific CDs markers. The positive result (peak fluorescence shift) for CD63 is green labeled, the positive result for CD81 is red labeled. These results were compared with EVs incubated only with beads (gray). e) Average diameter (140 nm) made by the Zetasizer instrument. f) Transmission electron microscopy (TEM) images by direct examination, showing purity hAT-MSC-derived EVs (black arrow); MET JEM 1200 EXII, Magnification 200k, scale bar 100nm

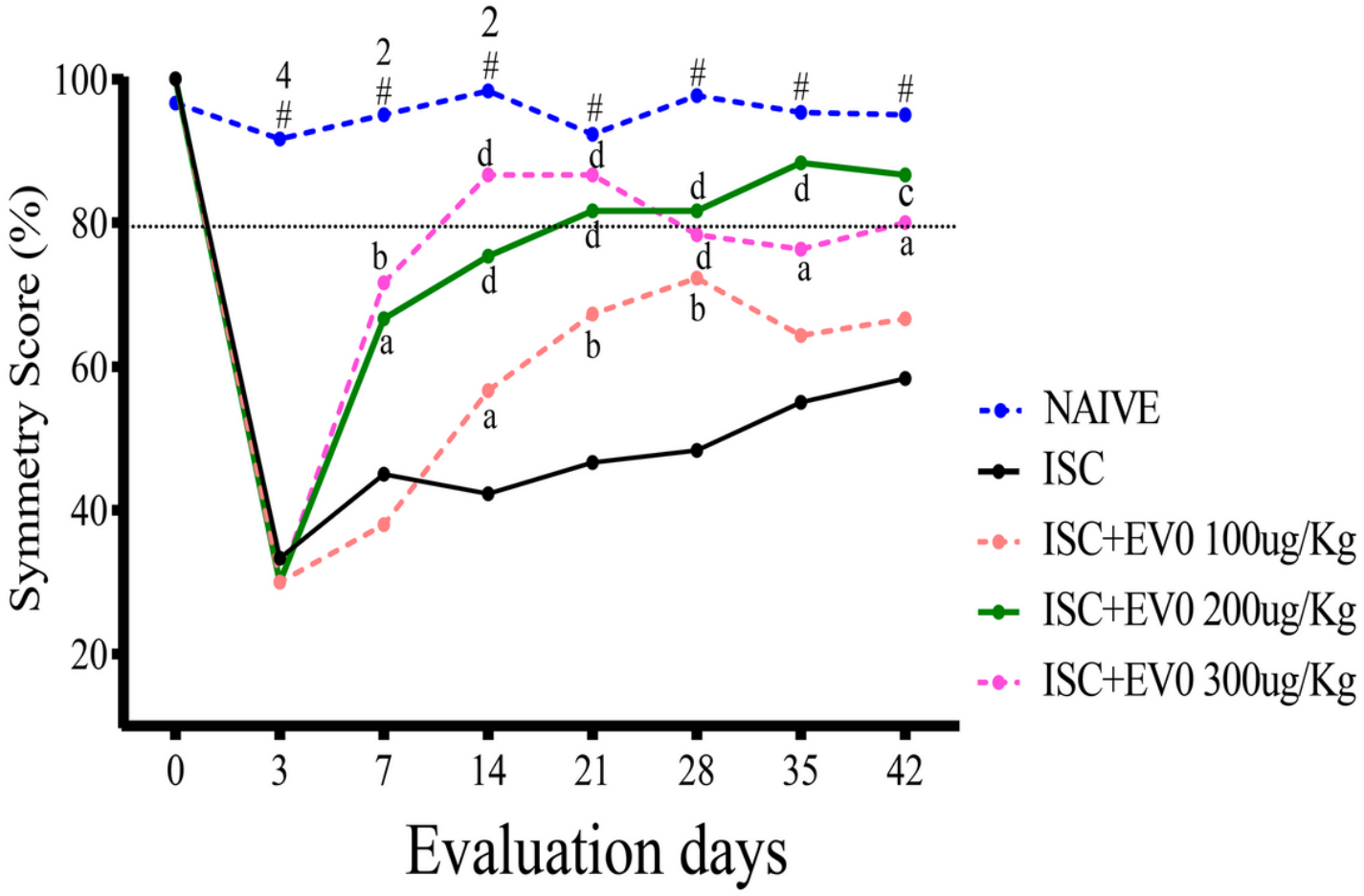

Figure 4

Dose curve for: Naive, ISC, ISC+EV0 100µg/kg, ISC+EV0 200µg/kg, ISC+EV0 300µg/kg, n = 3 for each group. Day 0 refers to baseline symmetry, evaluated 24 hours before induction of stroke. Data are expressed as mean (SD were less than 32% of respective mean) and analyzed by two-way ANOVA followed by Tukey's test: ap < 0.05, bp < 0.01, cp < 0.001 and dp < 0.0001, compared to the ISC group; 2p < 0.01, 4p < 0.0001, compared to 200µg/Kg and 300µg/Kg group. #p<0.01 compared to 100µg/Kg

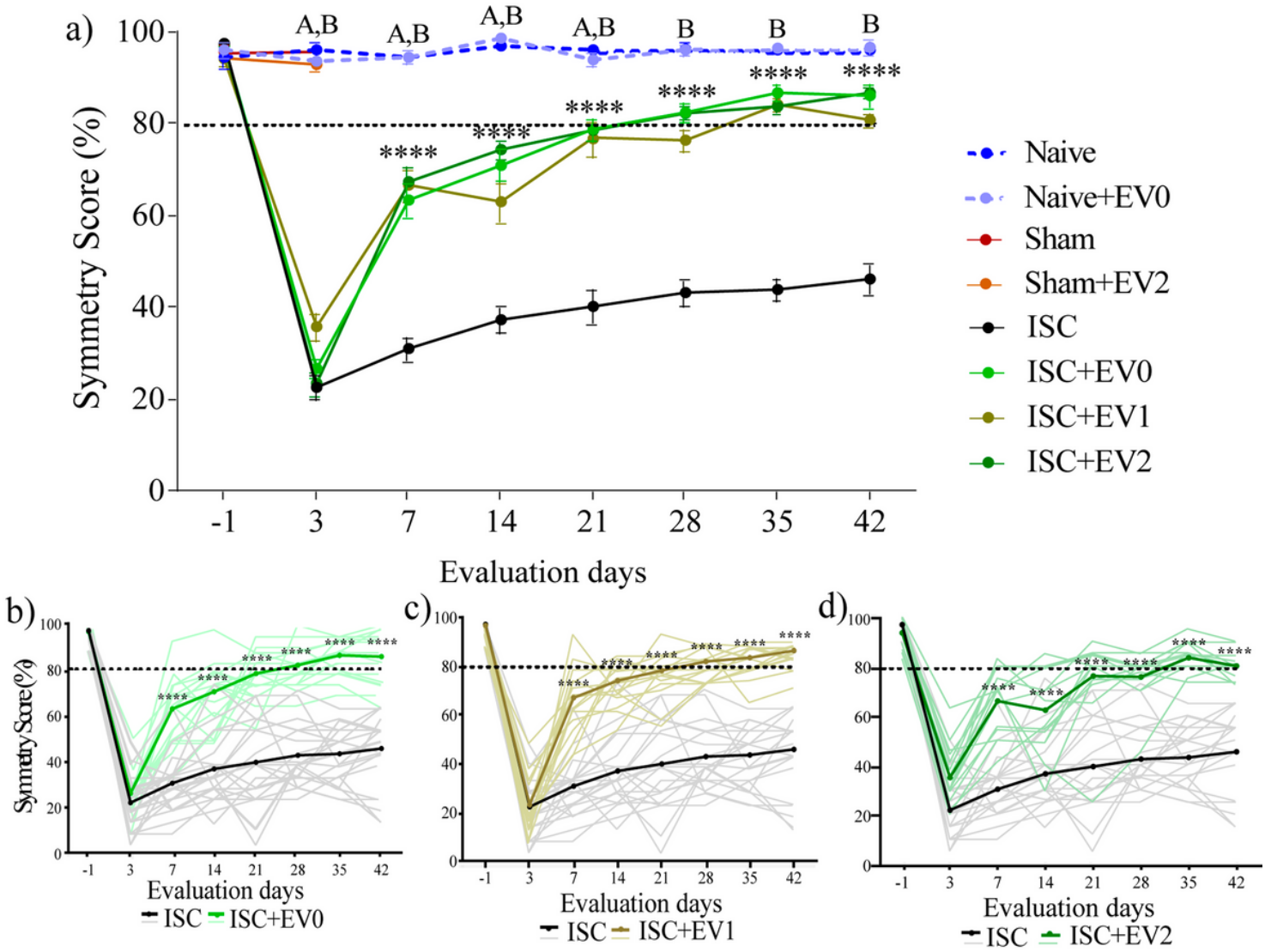

Figure 5

Symmetry score. a) The results are represented as group mean ± SEM. b - d) The individual results are represented as group mean (dotted line and strong lines) and individual performances (soft lines). b) ISC + EV0 group compared to the ISC group. c) ISC + EV1 group compared to the ISC group. d) ISC + EV2 group compared to the ISC group. Naive (n=8), Naive+EV0 (n=6), Sham (n=11), Sham+EV2 (n=5), ISC (n=22), ISC+EV0 (n=17); ISC+EV1 (n=17); ISC+EV2 (n=17). Data are expressed as mean ± SEM, analyzed by two-way ANOVA followed by Tukey's multiple comparisons test; ****p<0.0001, compared to ISC group; Ap<0.05, p<0.01, p<0.001 or p<0.0001 Naive group compared to ISC+EV groups and Bp<0.05, p<0.01, p<0.001 or p<0.0001 Naive group compared to ISC group

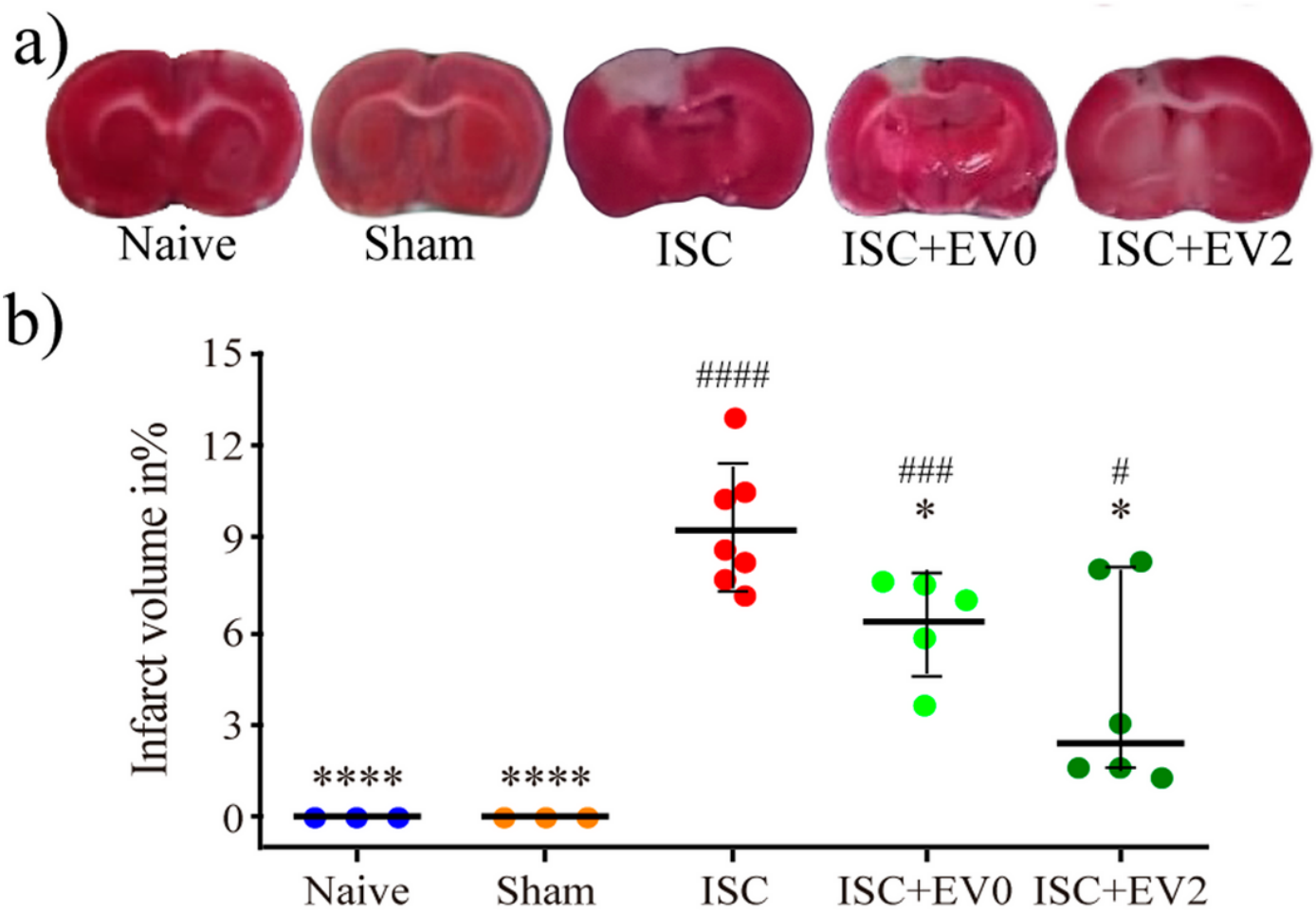

Figure 6

a) Representative images of the infarct volume (TTC staining). b) EVs treatment significantly decreases the infarct volume. For Naive, Sham, ISC and ISC+EV0 we used Statistical analysis by Unpaired T-test. Data are reported as mean ± SD, *p<0.05, ****p<0.0001 comparing to ISC group, ###p<0.001 and ####p<0.0001 comparing to Naive and Sham groups. For ISC+EV2 we used Mann-Whitney test of Unpaired t test. Data are reported as the median with interquartile range. *p < 0.05 comparing to ISC and #p<0.05comparing to Naive and Sham groups

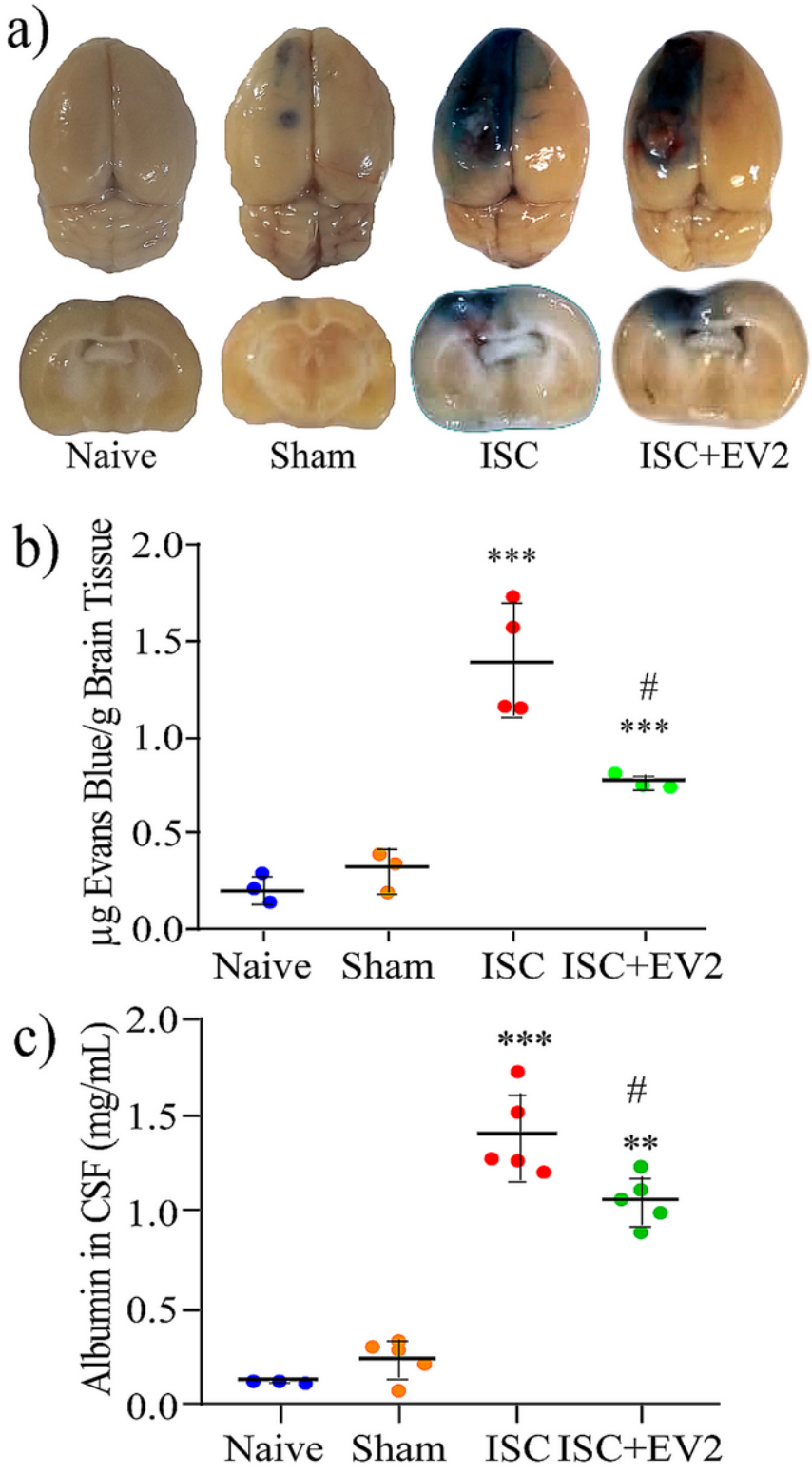

Figure 7

a) Representative images of Evans blue in brain tissue; dye crosses the BBB in Sham and stroke animals. b) Colorimetric quantification of brain Evans blue. c) Albumin levels in CSF. Statistical analysis by Unpaired t test. Data are reported as the mean ± S.D. **p<0.01 and ***p<0.001 comparing to Naive and Sham groups, #p<0.05 comparing to ISC group

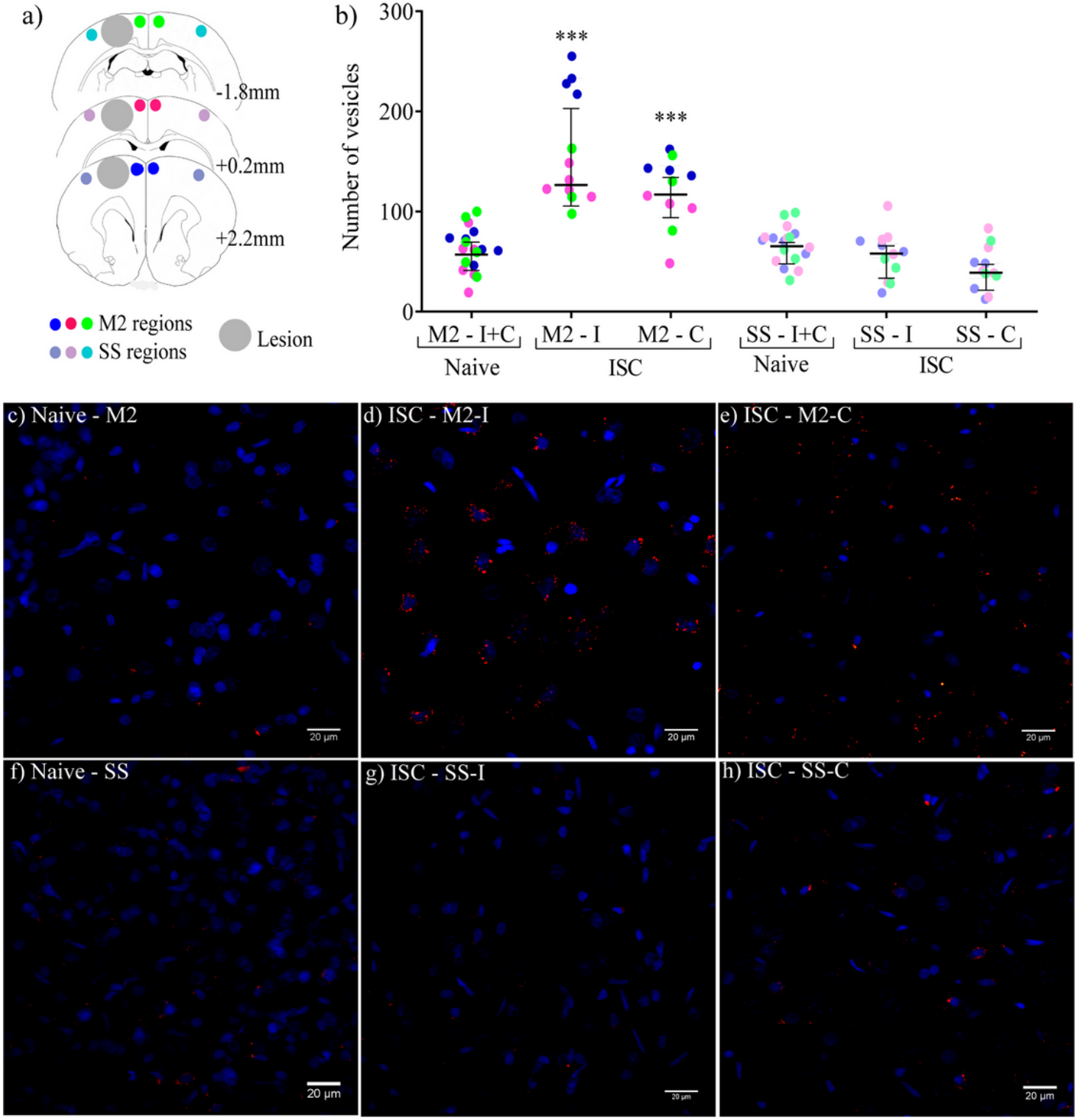

Figure 8

EVs distribution in brain cortex 18 hours after treatment. a) In a schema of the regions where the images were taken: peri-infarct region and its contralateral equivalent, supplementary motor cortex regions (M2) and somatosensory regions (SS) (+2.20mm, 0.2mm and -1.88mm to Bregma), Gray=lesion. b) Graph indicating greater number of vesicles in the ipsilateral M2 region; In c) – h) representative images of the M2 and SS regions located at 0.20mm from Bregma. c) naive M2; d) M2 ipsilateral perinfarct region; e)

M2 contralateral perinfarct region; f) naive SS region; g) SS ipsilateral perinfarct region; h) SS contralateral perinfarct region. Counting the EVs was performed using ImageJ software. Statistical analysis by Mann Whitney test. Data are reported as the Medians and interquartile ranges. ****p < 0.0001 comparing M2-I and M2-C to all other groups, N=3, 3 sections in each rat per group. Scale bars: 20μm

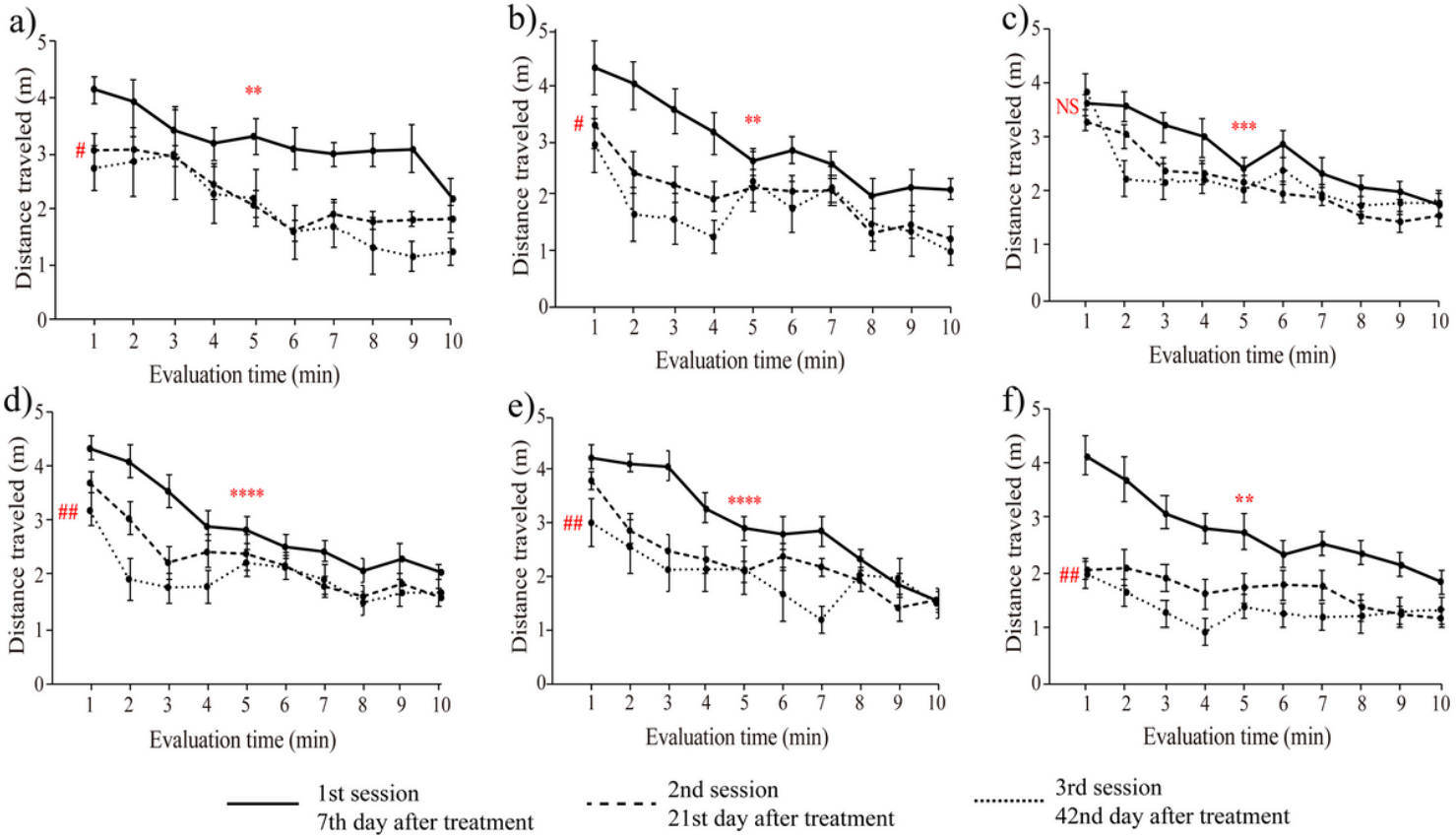

Figure 9

Open Field Task. Groups: a) Naive (n=8), b) Naive+EV0 (n=6), c) ISC (n=16), d) ISC+EV0 (n=16), e) ISC+EV1 (n=15) and f) ISC+EV2 (n=16). Statistical analysis by 2way ANOVA, followed by Tukey's multiple comparisons test. Data are reported as mean ± SEM. **p<0.01, ***p<0.001, compared the 1st with 5th minute of the same session; #p<0.05, ##p<0.001, compared the 1st minute of the first session with the 1st minute of the second/third or third sessions

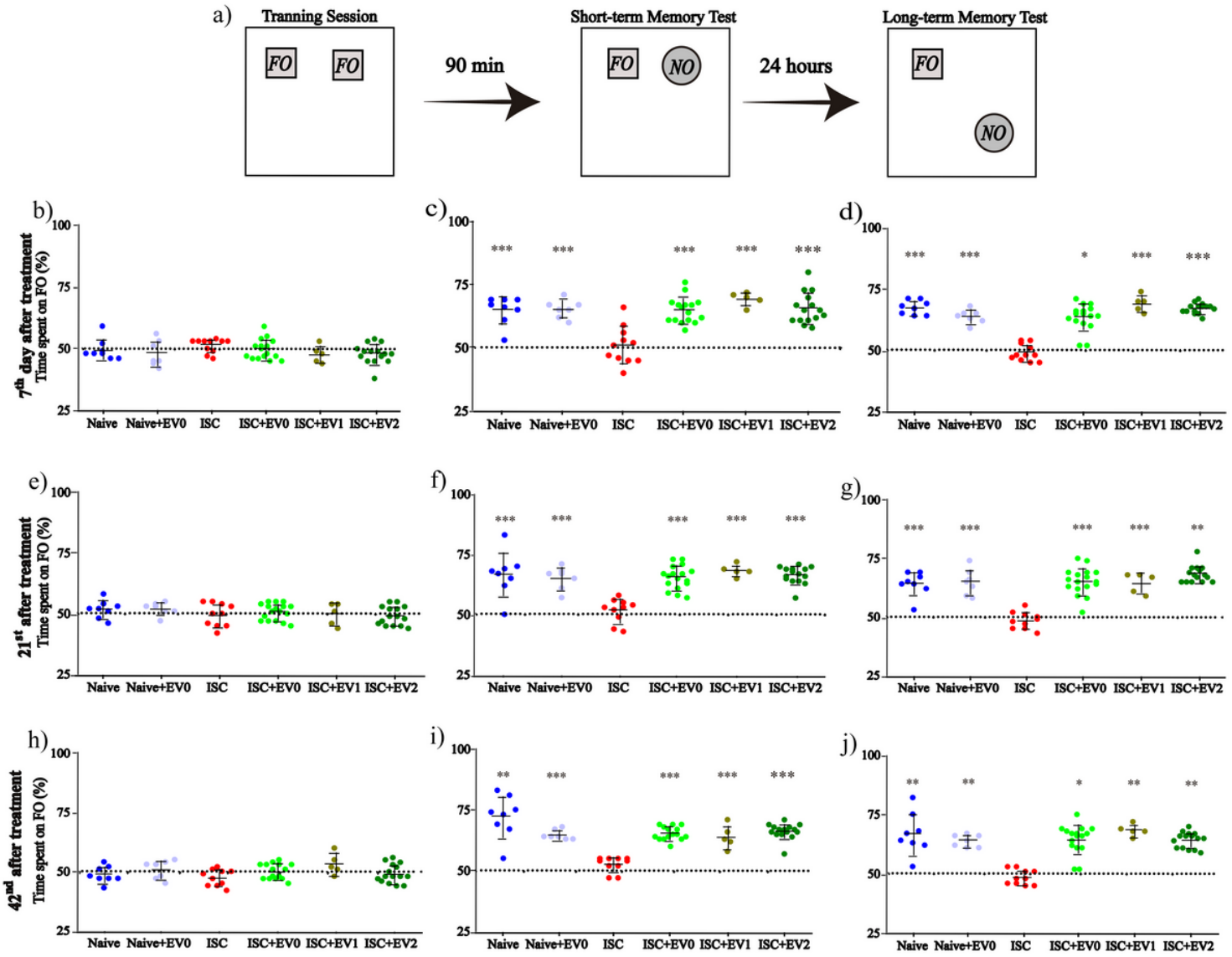

Figure 10

a) Scheme of protocol by using Familiar Object (FO) and/or Novel Object (NO). Groups: Naive (n=8), Naive+EV0 (n=7), ISC (n=16), ISC+EV0 (n=16), ISC+EV1 (n=5) and ISC+EV2 (n=16). Training sessions (TS) using 2 FOs; Short Term Memory test sessions 90 minutes after and Long Term Memory test sessions 24 hours after TS. b, e and h) 3 successive training sessions; c, f and i) 3 successive test STM sessions; d, g and j) 3 successive test LTM sessions. Unpaired T-test with theoretical average of 50%. Data reported as mean ± SD; *p<0.05, **p<0.01 and ***p<0.001, comparing to theoretical average of 50%

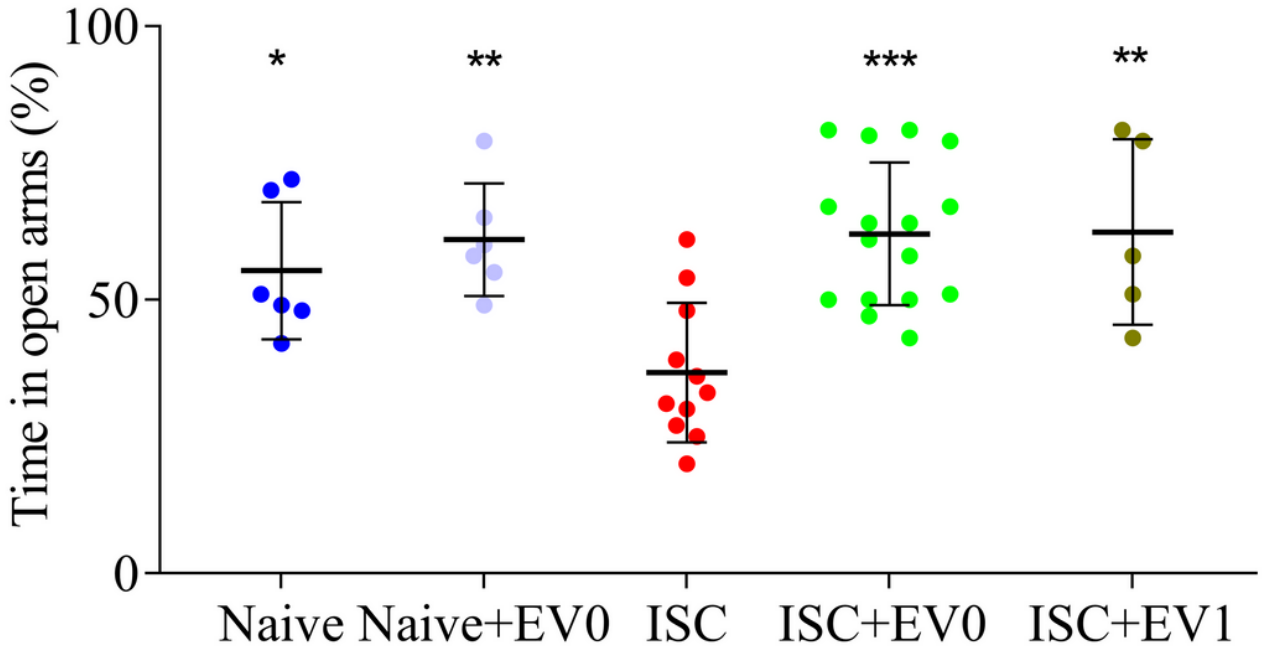

Figure 11

Elevated plus-maze task. Groups: Naive (n=6), Naive+EV0 (n=6), ISC (n=11), ISC+EV0 (n=16) and ISC+EV1 (n=5). Statistical analysis by Unpaired T-test. Data are reported as mean ± SD, *p<0.05, **p<0.01, ***p<0.001, compared to ISC group

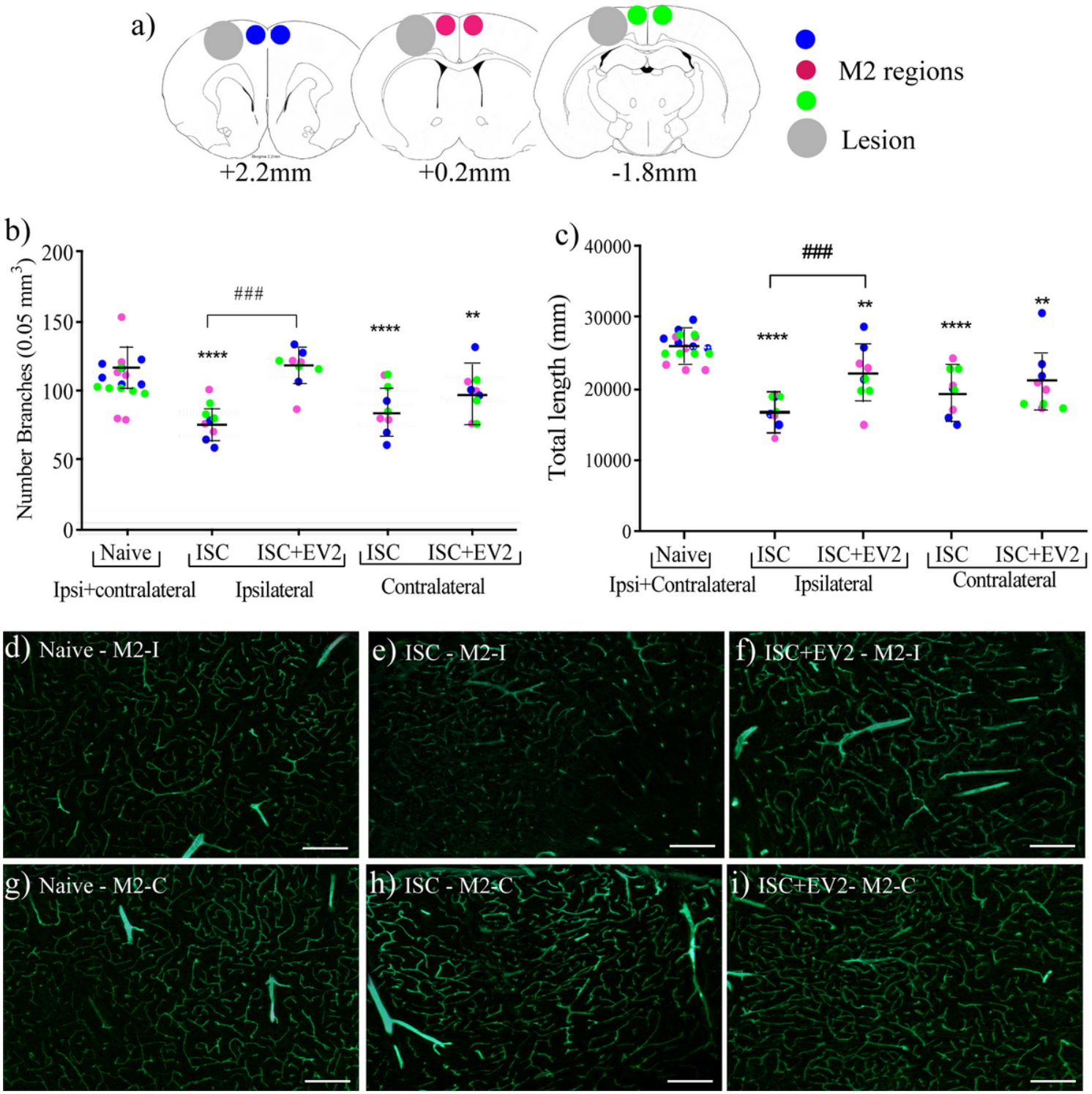

Figure 12

Analysis of blood vessels. a) a scheme of the regions where the images: peri-infarct region and its contralateral equivalent (+2.20mm,+ 0.2mm and -1.88mm of Bregma); b) Number of branches of the M2 regions; c) Total length of the M2 regions; d - i) Representative images of the M2 regions located at +0.20mm from Bregma: d) Naive M2 ipsilateral region, e) ISC M2 ipsilateral region; f) ISC+EV2 M2 ipsilateral region; g) Naive M2 contralateral region; h) ISC M2 contralateral region; i) ISC+EV2 M2 contralateral region. Statistical analysis by Unpaired T-test. Data are reported as the mean ± S.D. ****p <

0.0001 comparing to naïve group, ###p < 0.001 comparing ISC group. N=3, 3 sections in each rat per group. Scale bars: 20μm

Supplementary Files

This is a list of supplementary files associated with this preprint. Click to download.

- Supplementaryinformation1.mp4
- SupplementaryInformation2.pdf